技術論文

Predictive Simulation of PFI Engine Combustion and Emission

Hisashi Goto　Takeshi Morikawa　Mineo Yamamoto　Minoru Iida

当論文は、SAE 2013-32-9169 / JSAE 20139169として、台北(台湾)にて行われたSETC2013(Small Engine Technology Conference)にて発表され、High Quality Presentation Awardを得たものです。

DOI:10.4271/2013-32-9169

要旨

近年のコンピュータの発展およびエンジンにおける原理原則の研究解明により、3次元流動・燃焼シミュレーションを用いたエンジン開発の可能性が高まっている。これが可能になれば、試作・実験等の行程を減らせ、コスト削減・開発の短期化が達成できるだけでなく、計測不可能な現象やその要因を可視化できることから、開発の高効率化も見込める。これらの利点から、我々はこのシミュレーション、3次元CFD(Computational Fluid Dynamics)を開発フローに折り込むことを目的とし、そのツール化と高精度化、および突合せのための高度な計測を行ってきた。これまでのシミュレーション開発の結果、複数の条件において短時間で燃焼パターンおよび排ガスを精度良く予測できることを確認したので、これについて紹介する。

Abstract

This paper reports a methodology to estimate combustion pattern and emission by predictive simple simulation with good accuracy on various conditions of PFI engine. 3D-CFD cord VECTIS has been applied for this simulation, its settings and methods are as follows. RANS equation with liner k-epsilon model has been used as the turbulence model. Turbulent burning velocity equation contains not only turbulent velocity term but also laminar burning velocity term. For ignition model, we use a predictive model called DPIK. We iterate cycle calculation until wallfilm behavior is stabilized to get the reasonable mixture formation. We have applied this methodology to 125cc engine of motorcycle. As a result, we have obtained heat release curve and pressure curve with good accuracy on various operating conditions such as engine speed, engine load, air fuel ratio, wall temperature, and spray direction. CO and NOx calculated simultaneously have also been acceptable. CO formation is based on chemical equilibrium, and NOx formation is based on the extended Zeldovich mechanism. Using these results obtained by this methodology, optimal air-fuel distribution that affects heat release pattern and emission formation is suggested.

1 INTRODUCTION

Motorcycle is an important means of transportation for people in many nations and regions, so its improvement for high efficiency and low emission is demanded very much.

But the engine of motorcycle has many limitations about cost and space, compared to automobile.

Currently, development of computer and investigation of engine logics will make determination of engine design by 3D simulation possible. By using simulation, one can save cost, time, and labor such as trial and error in experiment. And also effective development is expected by visualization of cause and effect that cannot be measured. Practical examples of simulation have been reported such as consideration of optimal engine layout of DI engine[1], estimation of combustion and unburned HC by own detailed flamelet model[2], etc. And also we can find some reports of prediction of cyclic variation by LES.

Motorcycle has many engine types and also each one has special layout of parts such as intake pipe, fuel supply, etc. so the development of optimal options is needed for each of them in limited time. Therefore, simulation for motorcycle demands simpleness to obtain a result in short time, and enough accuracy on various conditions. And for PFI engine that is becoming more common for motorcycle, simulating wallfilm behavior in intake parts is important to estimate the reasonable air-fuel distribution that affects heat release pattern and emission formation in an engine cylinder. There are some experimental reports about wallfilm for PFI engine, such as measurement of wallfilm thickness on the intake port wall[3], observation of spray and wallfilm behavior in a simple test rig[4-6], and so on. They help not only understanding of experimental logics but also improvement of simulation.

We have developed methodology to estimate combustion pattern and emission by predictive simple simulation with good accuracy on various conditions of PFI engine. As a result, we have confirmed its accuracy by calculated parameters such as heat release curve, pressure curve, and emission formation of CO and NOx on some operating conditions of 125cc single cylinder engine that is global major product because of its good balance between power, simplicity, and cost. We introduce this methodology in this paper.

2 SIMULATION MODEL

2-1. FLOW

To obtain an individual result in a case in short time, the RANS equation with liner k-epsilon turbulence model has been used in our simulation. Flow distribution is affected by mesh size. Finer mesh makes results more accurate and independent from mesh size, but calculation time longer. We had compared simulated flow with PIV and LDA results, and then we decided mesh size as fine as we cannot expect more improvement with finer mesh.

2-2. SPRAY

DDM is used to represent spray behavior. Rosin-Rammler distribution is used as the initial droplet size distribution of the injected spray. Quantitative droplet distribution in the spray corn is represented by the normal distribution. Both distributions are validated with the experimental data of LDSA measurement.

Fuel property is one of the most important factors to deal with fuel behavior. Gasoline contains a lot of components, therefore it takes too much time to solve behavior of all components individually in simulation. In the other hand, property of the fuel changes according to the evaporation because lighter components tend to evaporate earlier and heavier components remain longer. So we assume rather simple multi-component fuel model. This model approximates the fractional boiling of the real multi-component fuels through the variation of the mean molecular weight of the evaporating fuel during the evaporation process based on the fuel distillation data. Characters of gasoline, such as viscosity, specific heat capacity, etc. are determined based on the instantaneous molecular weight. Distillation curve of gasoline at atmospheric pressure shown in Fig.1 has been determined by validation with experimental data. Fig.2 shows modeled molecular weight change of gasoline. Using this model, behavior of gasoline is estimated reasonably.

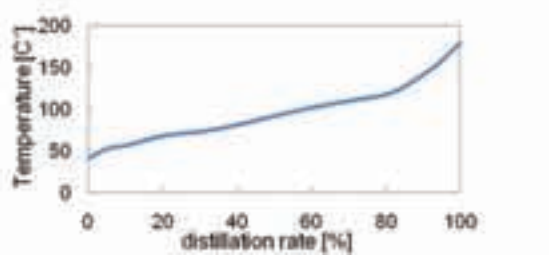

Figure 1: Distillation curve of gasoline

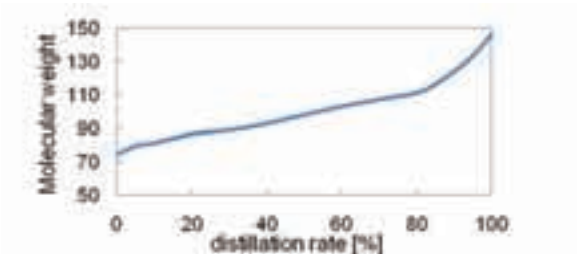

Figure 2: Modeled molecular weight change of gasoline

In order to simulate fuel wallfilm in operation, we iterate cycle calculation until wallfilm behavior is stabilized(Fig.3). In this way, we can obtain reasonable air-fuel distribution in engine steady state.

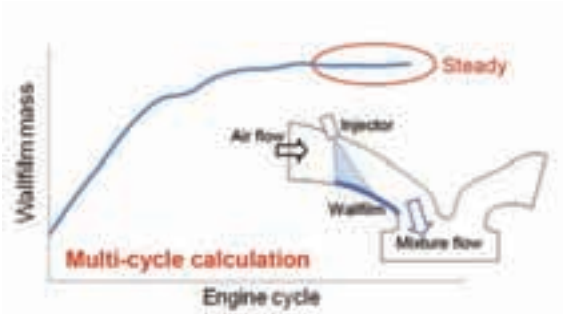

Figure 3: Methodology of steady state wallfilm modeling

2-3. INITIAL AND BOUNDARY CONDITION

For initial and boundary conditions, we have applied 1D simulation results. Its air and fuel mass that flowed into cylinder, and pressure histories have been adjusted to experimental results to evaluate reproducibility of 3D simulation precisely. As a result of multi-cycle calculations, error of air and fuel mass that flowed into cylinder model has been less than 1% from experiment.

2-4. FLAME PROPAGATION

Flamelet model is applied to flame structure. Turbulent burning velocity in our model contains not only turbulent velocity term but also laminar burning velocity term to represent the effect of fuel and residual gas distribution in an engine cylinder. Turbulent burning velocity equation is given by

$$S_T = S_L \cdot \left(1 + A \cdot u'^B\right) \quad (1)$$

Where S_L is the laminar burning velocity, u' is the turbulent velocity, A and B are adjustment factors. These factors have been validated by comparison of the heat release rate obtained by simulation with experimental data. A simple predictive model called DPIK[7] is used as ignition model. This simulates thermal expansion of flame kernel considering gas condition (laminar burning velocity, and turbulent velocity) until it reaches the order of integral length scale. This model is independent from mesh size.

3 CONFIGURATION MODELING

We applied this simulation to 125cc single cylinder engine. Its specifications are in table1. The geometry modeled contains configuration from throttle valve to outlet of exhaust port. One of the issues to consider is the direction of spark plug, location of side electrode. It is not usually controlled in the manufacturing process. We have checked its effects on combustion. Fig.5 shows simulated flame kernel expansion in each spark plug direction as shown in Fig.4 on a same operating condition. Side electrode of spark plug absorbs flame kernel energy, thus avoid kernel expansion. It also changes flow distribution in the cylinder. These effects appear notably in this simulation that outputs ensemble-averaged results by 1 cycle calculation.

So we have compared this with experiment under a typical partial load condition to investigate its effect level of this engine. 500 cycles experiments were done 3 times for each plug direction in a condition of Case1(IMEP CoV 1%) is shown in table2. Fig.6 shows the deviations of 0-10% burn duration from a result of plug direction 0deg in each direction of experiment and simulation. According to this result, we think the effects of plug direction in experiment are small enough to be ignored. We think that this difference is because the tiny velocity-distribution around the plug that cannot be simulated occurs in experiment. In reality, the transportation and expansion of small flame kernel is sensitively affected by velocity field with small scale near the spark plug. The velocity fluctuates between each cycle. This causes cycle-variation of flame propagation. Heat release obtained by averaging the data in many cycles, therefore, is the cycle-average of flame propagation fluctuated by the velocity. On the other hand, velocity with small scale in simulation is treated as turbulence which has no direction. Velocity near the spark plug, affected by the location of the side electrode, determines the direction of propagation. Therefore the location of the side electrode is more directly affected to the heat release.

As a result, we have decided to remove side electrode model in simulation, and fixed some calculation parameters. But this

comparison between experiment and simulation showed some correlations. So there is a possibility that we can decide optimal plug direction by this simulation.

Table 1: Engine specification

Engine Type	4-Stroke, 2-Valve, Single Cylinder, Air-Cooled
Bore×Stroke	52.4×57.9 mm
Displacement	125 cc
Fuel supply	Port Fuel Injection

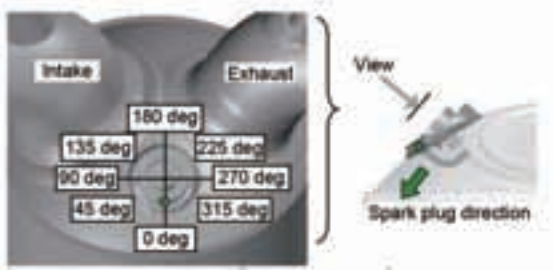

Figure 4: Spark plug(side electrode) directions

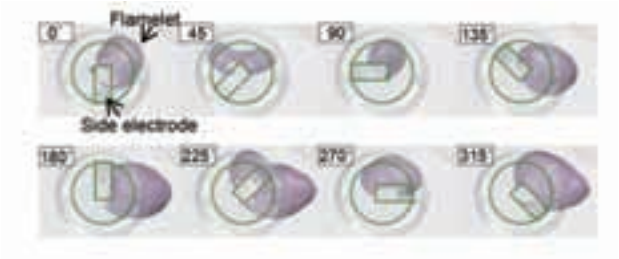

Figure 5: Simulated flame expansion (effect of plug direction)

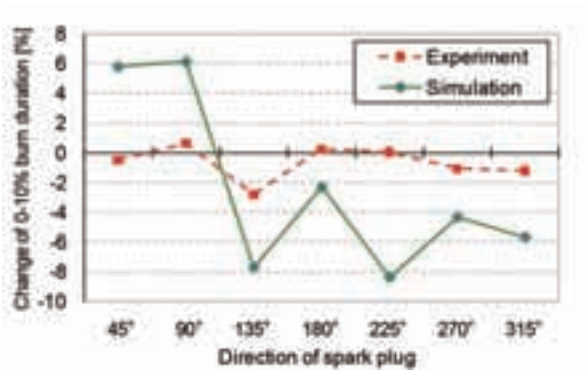

Figure 6: Deviation of burn duration from plug direction 0deg

4 OPERATING CONDITIONS

As shown in table2, we have applied this simulation to 8 operating conditions to check how it behaves with different engine speed, engine load, air fuel ratio, wall temperature, and spray direction. The conditions of cooler wall temperature and spray direction toward intake port wall are mainly intended to confirm reproducibility of simulation in conditions that much wallfilm is generated. Configurations of injection are shown in Fig.7. Ignition timing is set as MBT in each condition.

Table 2: Engine operating conditions

Engine rpm	3,500					4,400	4,000	3,000
Engine Load	Road Load						Full Load	
Air-Fuel Ratio	14.5			13	16	14.5	12	
Injector sprays toward	valve		port-wall	valve				
Oil Temperature	Hot	Cool	Hot					
Case No.	1	2	3	4	5	6	7	8

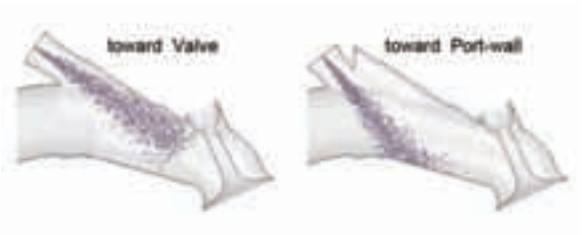

Figure 7: Configuration of injection

5 RESULTS

5-1. FLOW & SPRAY

Accuracy of simulated wallfilm was confirmed by some ways. Fig.8 shows comparison of wallfilm behavior between simulation and experiment observed by borescope in Case3(spray toward port-wall). Two position markers in both simulation and experimental images indicate the same location on each image. Methodology of the experiment was described more in detail in [8]. The order of the cycle indicates the number of the cycle from the start of the injection after motoring operation. All images are at the IVC timing after injection. The measured temperature of walls in a steady state have been applied to ones of simulation. At 1st cycle, thin wallfilm are distributed from the joint to before lower marker in experiment. Similar wallfilm can be seen in simulation result. Wallfilm reaches valve after some cycles in both simulation and experiment. The cycle is 4th in simulation, though 8th in experiment. This means that wallfilm in simulation expands a little faster than that of experiment. We think that is because the effect of wall surface roughness is not well simulated. However, this simulation seemed to be able to estimate steady state wallfilm distribution in comparison of wet area.

To confirm validity of air-fuel distribution in the cylinder, fuel concentration near the spark plug has been measured by infrared laser absorption method. Fig.9 shows equivalence ratio histories around spark plug in the Case1 and Case8. Experimental results are ensemble-averages of 200 cycles. In both cases, mixture is rich just after the overlap TDC, and it becomes lean during the intake stroke. It becomes near stoichiometry after BDC. This trend can be seen in simulation and experiment, though there are discrepancies quantitatively. Therefore, we think simulated air-fuel distributions are reasonable, while it still needs more effort to better simulate.

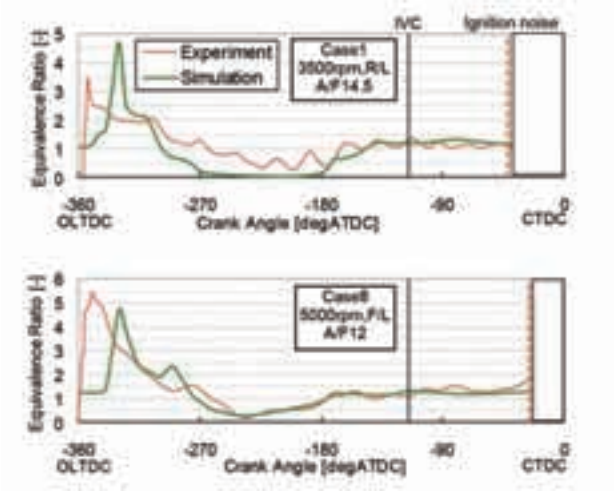

Figure 9: Equivalence ratio histories at spark plug

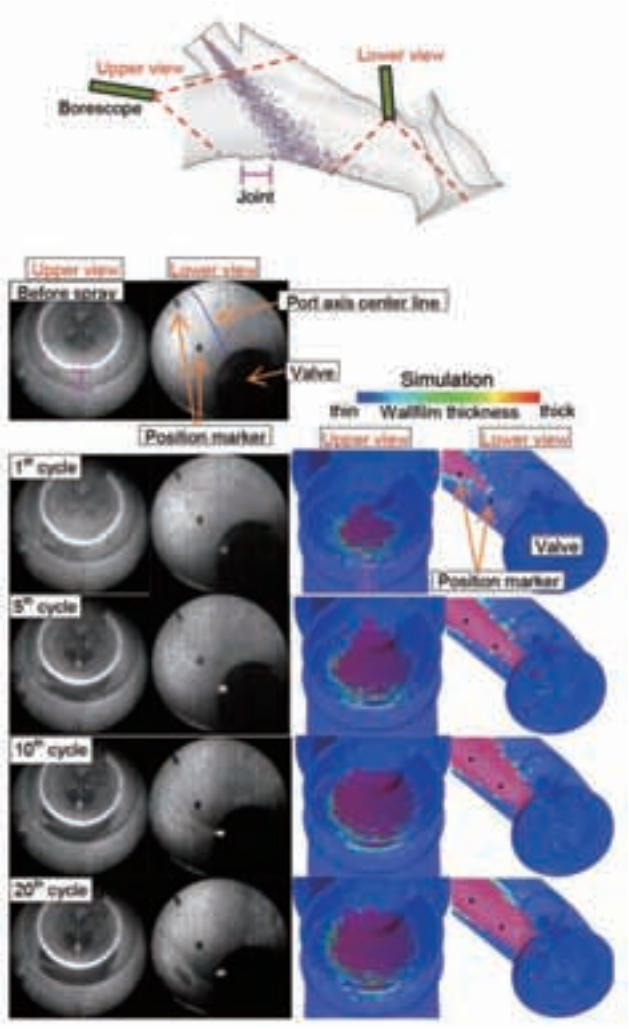

Figure 8: Comparisons of wallfilm behavior

5-2. COMBUSTION

Fig.10(a)(b) shows calculated(by same adjustment factor) and measured heat release rates and pressure curves in the all cases. And Fig.11 shows correlations of those heat release. Experimental results are cycle-averages of 500 cycles. Initial flame propagations have been estimated with good accuracy, and the errors of 0-10% burn duration are less than ±10% in the all cases. In cases of road load conditions (Case1~Case6), main heat release and pressure curves have also been estimated with good accuracy, so one can see this simulation is applicable to various engine conditions. On the other hands, in cases of full load conditions (Case7 and Case8), heat release continues longer especially at later part in simulation than in experiment. One of the reasons explain this result is turbulence under WOT condition is smaller in simulation than in experiment, and then turbulent burning velocity become lower. Other factors such as distribution of A/F, that of temperature, and that of residual gas may not be the reason because they are almost homogeneous in this condition(Fig.12). So we have to consider about introduction of other turbulence model, or build some equations to avoid getting this error. Anyway, we have confirmed this predictive simulation can estimate heat release pattern and pressure curve with good accuracy on various engine conditions.

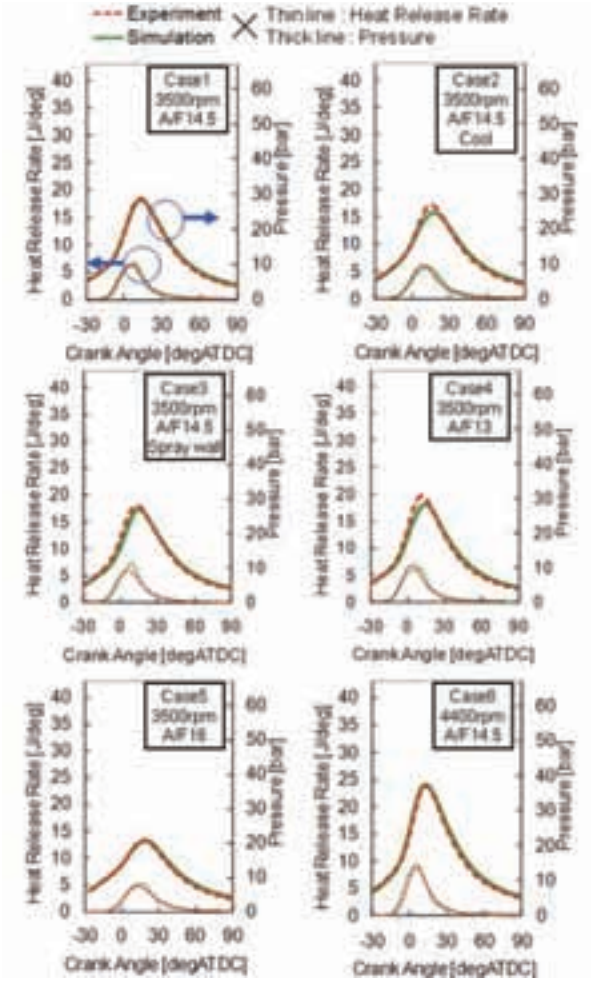

Figure 10(a): Comparisons of heat release & pressure curves

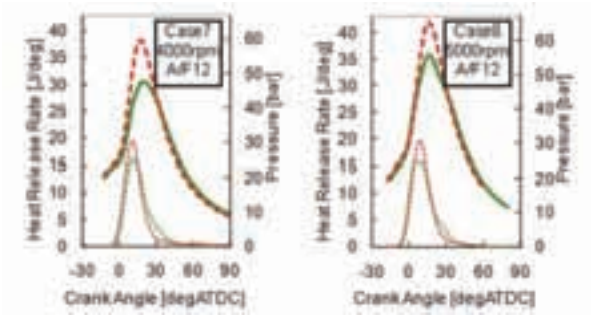

Figure 10(b): Comparisons of heat release & pressure curves

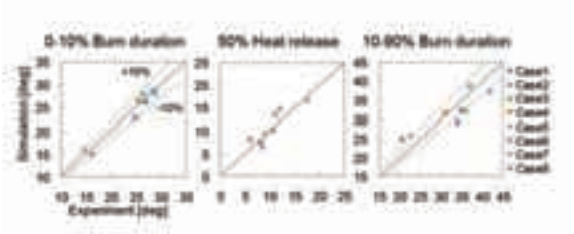

Figure 11: Correlations between experiment and simulation

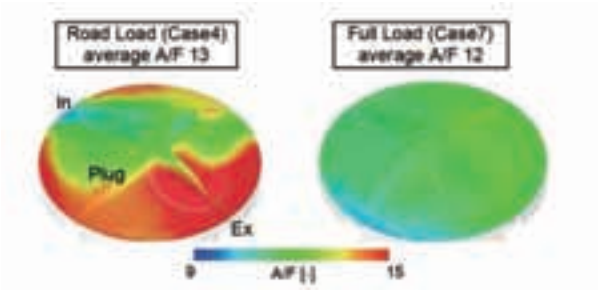

Figure 12: Comparison of A/F distribution at TDC

5-3. EMISSION

During combustion simulation, CO and NOx are calculated simultaneously. CO formation is modeled very simply based on chemical equilibrium during combustion in each cell. NOx formation is modeled based on the well-known extended Zeldovich mechanism.

We have confirmed reproducibility of CO and NOx calculated by these simulation models. First, heat release pattern has been suited to experiment as much as possible by changing adjustment factors of burning velocity in each case. As a result, emissions obtained are shown in Fig.13 and Fig.14. Experimental results are engine out emission in front of the catalyst, and simulation results are their fractions in the cylinder at the end of heat release. We assume oxidation reaction of products after heat release in the cylinder negligible in the experiment. Comparison of CO concentration shows good accuracy even with chemical equilibrium. This indicates CO formation is able with depends on average A/F. Average of absolute errors was 0.3vol%. Comparison of NOx concentration also shows tendency of each experimental result. Average of absolute errors was 610volppm. NOx formation is mainly determined by A/F and temperature distribution, and their history because the reaction rate is slower than the change of the physical condition. As well-known, more lean A/F and higher temperature cause more NOx formation. One can see the example of that tendency between results of Case1, Case2, and Case6, assuming that those internal gas are homogeneous. In the same A/F conditions, lower NOx formed in Case2 than in Case1 because of its lower temperature condition, and more NOx formed in Case6 than in Case1because of its higher temperature condition caused by higher heat release.

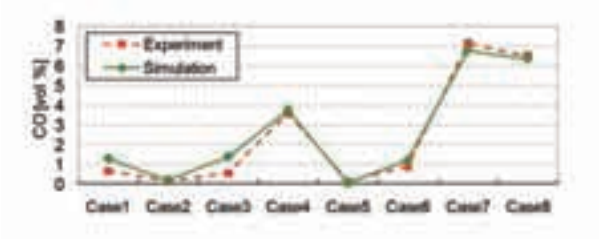

Figure 13: Comparisons of CO fractions

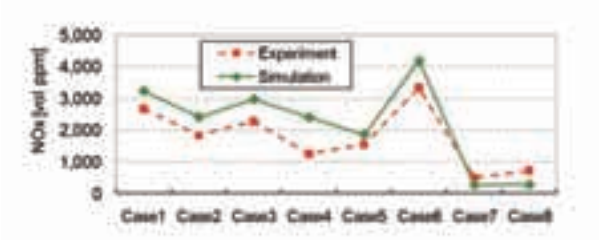

Figure 14: Comparisons of NOx fractions

5-4. CONSIDERATION OF INTERNAL GAS DISTRIBUTION TO AFFECT THE NOx FORMATION

Using these simulation results, effects of internal gas distribution on emission formation of NOx is discussed. Fig.15 shows distributions of NOx, A/F, and temperature in the Case1 at 15degATDC. We can see the temperature dependence of NOx(lower NOx fraction at lower temperature) at many places such as area A. But some area shows few NOx fraction at high temperature because of rich A/F such as area B. In order to evaluate more quantitatively though simply, their contributions are evaluated by initial NOx(NO) formation speed [9] based on Zeldovich mechanism, given by

$$\frac{d[NO]}{dt} = \frac{6\times10^{16}}{T^{0.5}}\exp\left(\frac{-69{,}090}{T}\right)[O_2]^{0.5}[N_2] \qquad (2)$$

Fig.16 shows initial NO formation speed in the case of Octane. [O2] and [N2] are calculated by chemical equilibrium. According to this, lean A/F causes high formation speed in a same temperature. In adiabatic temperature indicated by broken line, NO formation speed become fastest around stoichiometric condition. Actually, partly maximum temperature depends on not only A/F but also initial condition and combustion pattern. Using these properties of NO formation, we can expect to reduce NOx formation by some approaches.

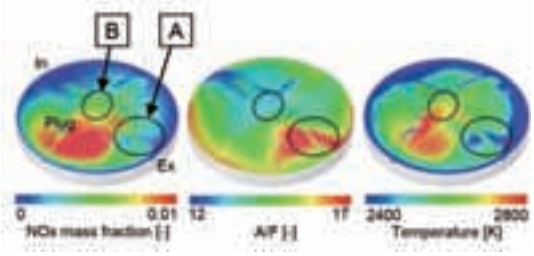

Figure 15: NOx,A/F,Temperature distributions in Case1 (15degATDC)

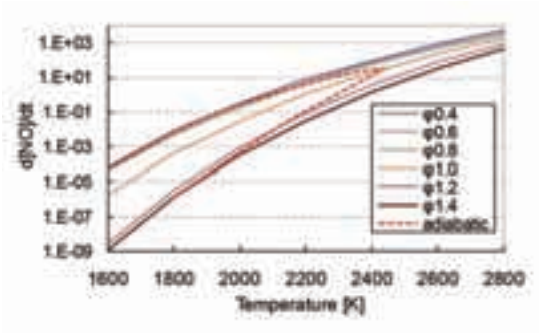

Figure 16: Initial NO formation speed

6 SUMMARY/CONCLUSIONS

We have developed a methodology of predictive simple simulation of in-cylinder phenomena, heat release and exhaust emission generation for PFI engine development. We have applied this methodology to air-cooled 125cc single cylinder engine and obtained conclusions as below:

- Combustion pattern by simulation shows good accuracy in various operating conditions such as engine speed, engine load, air fuel ratio, wall temperature, and spray direction.
- Concentration of CO and NOx emission calculated are also simulated accurately under the condition heat release pattern is accurate.
- Using these simulation results, effective air-fuel distribution to reduce NOx is suggested.

REFERENCES

1. K. Sato, Y. Ueki, Y. Wada, H. Hongo, Y. Miyauchi, H. Yokohata: Application of CAE to SKYACTIVE-G, Mazda Technical Review, No.29 (2011), p.47-52
2. A. Teraji, T. Tsuda, T. Noda, T. Kubo, T. Itoh: Prediction of Unburned HCs by Using Three-Dimensional Combustion Simulation in Spark Ignition Engines, Journal of the Combustion Society of Japan Vol.49 No.147 (2007), p.70-76
3. Y. Takahashi, Y. Nakase, Y. Katou: Analysis of the Fuel Liquid Thickness on the Intake Port and Combustion Chamber of a Port Fuel Injection Engine, Denso Technical Review, Vol.13, No.1 (2008), p.44-51
4. Y. Moriyoshi and M. Iida: Analysis of Port Injected Fuel Spray Under Cross Wind Using 2-D Measurement Techniques, SAE International Journal of Fuel and Lubricants December 2010 vol.3 No.2, p.1081-1092
5. G. Wang, C. Arcoumanis, M. Iida and Y. Motoyama: Characterisation of the Wall Fuel Film Development in a Simulated Engine Intake Port, The Seventh International Conference on Modeling and Diagnostics for Advanced Engine Systems (2008), p.461-467
6. M. Iida, K. Yoshikawa and H. Tanaka, G. Wang, C. Arcoumanis: Fuel Film Behavior Analysis Using Simulated Intake Port, SAE International Journal of Engines March 2010 vol.3 No.2, p.756-763
7. L. Fan, F. Li, Z. Han, R.D. Reitz: Modeling Fuel Preparation and Stratified Combustion in a Gasoline Direct Injection Engines, SAE Paper 1999-01-0175
8. M. Yumoto, K. Goto, S. Kato and M. Iida: Influence of Injection and Flame Propagation on Combustion in Motorcycle Engine - Investigation by Visualization Technique -, SAE 2011-32-0566
9. John B. Heywood: Kinetics of NO Formation, Internal Combustion Engine Fundamentals, United States of America, McGraw-Hill, Inc., 1988, p.572-577

ACKNOWLEDGMENTS

The authors would deeply thank Keiichi Yoshikawa, Miki Yumoto, Yoshihito Ito, Tsuneo Hayashi and all colleagues who contributed to this research.

DEFINITIONS/ABBREVIATIONS

DI: Direct Injection
HC: Hydrocarbons
LES: Large Eddy Simulation
PFI: Port Fuel Injection
CO: Carbon monoxide
NOx: Nitrogen Oxide
RANS: Reynolds-Averaged Navier-Stokes
PIV: Particle Image Velocimetry
LDA: Laser Doppler Anemometer
DDM: Discrete Droplet Model
LDSA: Laser Diffraction Spray Analyzer
DPIK: Discrete Particle Ignition Kernel
IMEP: Indicated Mean Effective Pressure
CoV: Coefficient of Variance
MBT: Minimum spark advance for Best Torque
IVC: Intake Valve Close
TDC: Top Dead Center
BDC: Bottom Dead Center
CTDC: Compression TDC
OLTDC: Over Lap TDC
WOT: Wide Open Throttle
A/F: Air/Fuel
ATDC: After TDC
NO: Nitric Oxide

■著者

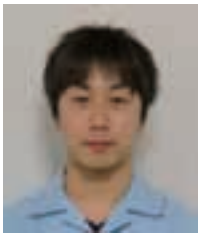

後藤 久司
Hisashi Goto
技術本部
研究開発統括部
基盤技術研究部

森川 健志
Takeshi Morikawa
技術本部
技術企画統括部
ﾃﾞｼﾞﾀﾙｴﾝｼﾞﾆｱﾘﾝｸﾞ部

山本 峰生
Mineo Yamamoto
退職

飯田 実
Minoru Iida
技術本部
研究開発統括部
基盤技術研究部